

SELF-CONSISTENT FULLY DYNAMIC ELECTRO-THERMAL SIMULATION OF POWER HBTs

F. Cappelluti¹, F. Bonani¹, S. Donati Guerrieri¹, G. Ghione¹, C.U. Naldi¹,
M. Peroni², A. Cetronio², R. Graffitti²

¹Dipartimento di Elettronica, Politecnico di Torino, Torino, Italy, bonani@polito.it

²Alenia Marconi Systems, Roma, Italy, mperoni@amsjv.it

ABSTRACT

A new self-consistent dynamic electro-thermal model for power HBTs is presented coupling a circuit-oriented electrical model, fitted on experimental data, with a full frequency domain thermal model. The thermal model provides the exact frequency behaviour of the device thermal impedance through a quasi-3D approach. The electro-thermal self-consistent solution is achieved, in large-signal periodic operation, through Harmonic Balance analysis. The model has been applied to the simulation of some HBT layouts from Alenia Marconi Systems.

INTRODUCTION

Heterostructure Bipolar Transistors (HBTs) have demonstrated promising performance for medium power microwave applications, and are characterized by a high current density, thus being able to handle large power densities. This, on the other hand, makes device self-heating a primary concern in device and circuit design, both in terms of reliability and performance optimization, thus requiring the availability of accurate and comparatively efficient electro-thermal models leading to a self-consistent analysis. Furthermore, in GaAs-based multifinger structures, owing to high dissipated power resulting in high junction temperature, thermal instabilities can arise, resulting in a dramatic performance drop in terms of both gain and bandwidth [1] (gain collapse phenomenon). This topic has been widely investigated; however, the electrothermal models and stability analysis techniques proposed in the literature are usually derived either in static conditions [1, 2] or exploit a possibly inaccurate single pole approximation of the device thermal impedance [3].

In this paper we present an original approach to HBT analysis wherein a self-consistent, fully dynamic electro-thermal model is exploited. The thermal behaviour of the device is described by means of the thermal impedance matrix approximation, which is evaluated for a given device layout by approximating each thermal source (i.e., each emitter of a multifinger HBT) through a superposition of spherical sources, thereby allowing for a closed form estimation of the frequency-dependent, dynamic thermal impedance. Concerning the electrical part, a circuit-oriented, dynamic large-signal model with temperature dependent parameters is exploited.

The model has been applied to the analysis of several device layouts for an Alenia Marconi Systems process aimed to develop power GaAs/AlGaAs HBTs. The occurrence of thermal instability (gain collapse), i.e. a sudden decrease of total collector current, has been observed, and interpreted as the result of the occurrence of a bifurcation process in the nonlinear, electrothermal model equations.

THE SELF-CONSISTENT DYNAMIC ELECTRO-THERMAL MODEL

Device self-heating can be studied by solving in a self-consistent way a model for the thermal behaviour and a set of equations describing the device electrical characteristics. Self-consistency is required since electrical dissipated power drives device heating, and the parameters of the electrical model are, in turn, temperature-dependent. In the following, we shall assume that the device is driven by large-amplitude, harmonic signals, represented as:

$$x(t) = \sum_q \hat{x}_q e^{j\omega_q t} \quad (1)$$

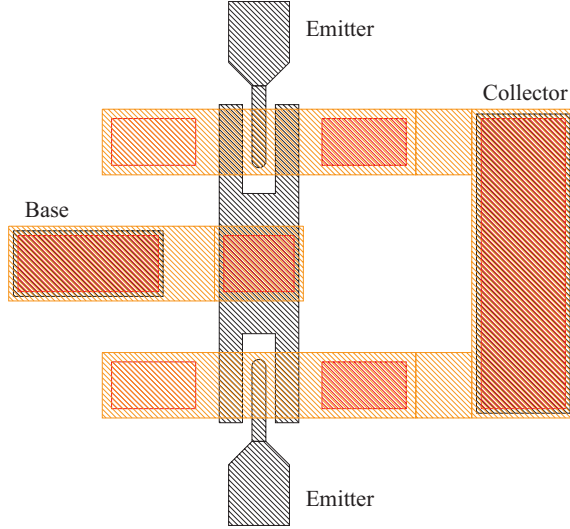


Figure 1: Layout of the 2 finger HBT.

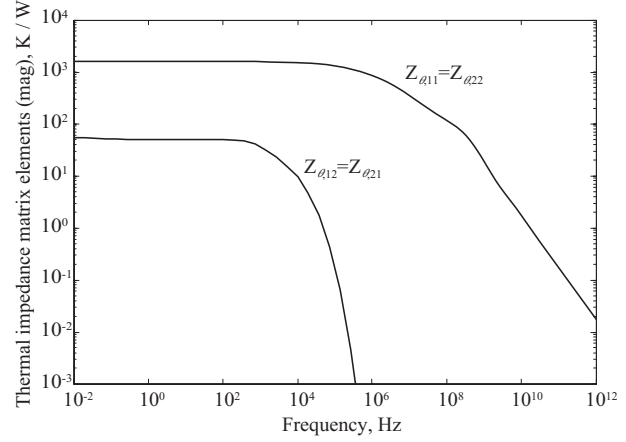


Figure 2: Frequency dependence of the thermal impedance (magnitude) matrix elements for a 2 finger HBT.

where $\omega_q = q\omega_0$ is the angular frequency of harmonic q and \hat{x}_q the corresponding amplitude. $x(t)$ can be either an electrical or a thermal variable.

Let us consider a N finger device, and let us denote each of them through the integer index k . The k -th finger temperature increase $\Delta T_k = T_k - T_0$ (T_0 is the heat-sink reference temperature) is a function of the device dissipated power. Let $p_{dk} = v_{CEk}i_{Ck} + v_{BEk}i_{Bk}$ be the (instantaneous) dissipated power on finger k . Within the thermal impedance approximation, one has:

$$\Delta \hat{\mathbf{T}}_k = \sum_n \hat{\mathbf{Z}}_{\theta, kn} \cdot \hat{\mathbf{p}}_{dn} \quad (2)$$

where $\Delta \hat{\mathbf{T}}_k$ is the vector of harmonic temperature increase amplitudes for finger k , $\hat{\mathbf{Z}}_{\theta, kn}$ is the thermal impedance matrix (in the frequency domain) between fingers n and k , and $\hat{\mathbf{p}}_{dn}$ is the vector of harmonic components of the dissipated power in finger n . The thermal impedance is evaluated directly in the frequency domain according to the analytical method proposed in [4], complemented by the application of the images method in order to recover the substrate thermal boundary conditions, see e.g. [5]. An example of frequency dependence for the elements of the thermal impedance matrix of a 2 finger power HBT (see Fig. 1 for the device layout, each emitter is $3 \times 15 \mu\text{m}^2$) is shown in Fig. 2, where the substrate thickness was $120 \mu\text{m}$ and the material (GaAs) thermal conductivity was $\kappa_{\theta} = 4.8 \times 10^{-5} \text{ W } \mu\text{m}^{-1} \text{ K}^{-1}$. Fig. 2 clearly shows that a single-pole approximation is rather poor, since the decrease rate is quite different from 20 dB/decade for both the diagonal and off-diagonal elements. As a general comment, one can observe that the thermal coupling between the fingers is, due to the layout spacing, quite low.

Concerning the electrical device behaviour, in DC operation a standard Gummel-Poon model for the forward operation of each device finger is adopted [6]:

$$i_{Bk} = \frac{I_{C0}}{\beta_{Fk}} \exp \left[-\frac{E_g(T_k)}{k_B T_k} \right] \left[\exp \left(\frac{v_{BEk}}{\eta_F k_B T_k} \right) - 1 \right] + I_{B0} \left[\exp \left(\frac{v_{BEk}}{\eta_E k_B T_k} \right) - 1 \right] \quad (3)$$

where E_g is the base material energy gap, η_F the ideality factor of the base-emitter junction, $I_{C0s} = I_{C0} \exp[-E_g(T_k)/(k_B T_k)]$ is the base-emitter reverse saturation current, η_E the ideality factor for the parasitic base current, I_{B0} represents such parasitic current in reverse saturation and $\beta_{Fk}(T_k) = \beta_0 \exp[\Delta E_v/(k_B T_k)]$ is the finger gain excluding parasitic base current. ΔE_v is the valence band discontinuity of the base-emitter junction. For time-dependent analysis, this DC model must be complemented by a dynamic part represented through (generally) nonlinear capacitances and a time delay between emitter and collector currents. The circuit extracted from measurements is shown in Fig. 3.

The electrical and thermal device models are finally combined in order to derive a set of nonlinear differential equations describing the multifinger device layout. For the sake of simplicity, Fig. 4 represents the equivalent electro-thermal circuit for a two-finger HBT. The resulting dynamic system is solved directly in the frequency domain by means of the Harmonic Balance (HB) method [7], thereby obtaining a self-consistent electro-thermal working point.

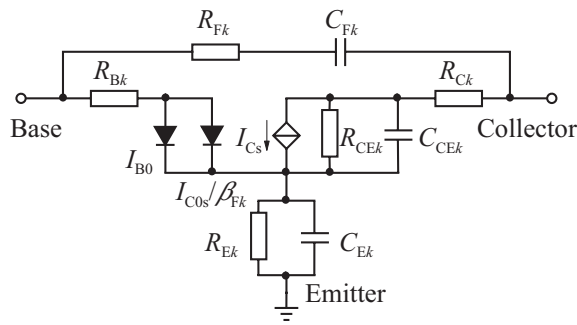


Figure 3: Electrical equivalent circuit for each HBT finger.

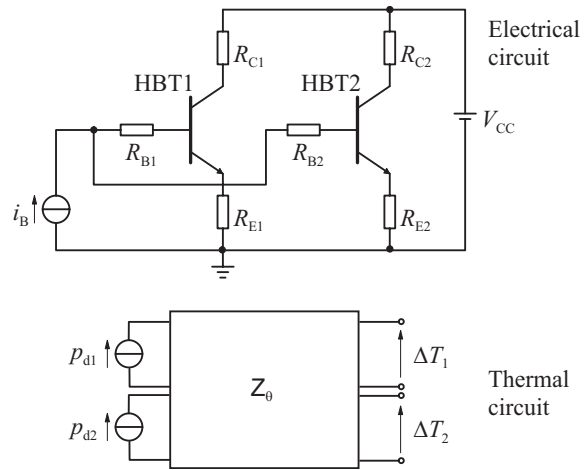


Figure 4: Electro-thermal equivalent circuit for a two-finger power HBT.

RESULTS

The model has been applied to the self-consistent simulation of the electro-thermal properties of three different layouts for the same Alenia Marconi Systems process, corresponding to 2 finger, 4 fingers and 8 fingers devices. The electrical model has been fitted against small-signal (see Fig. 5) and DC [8] measurements, with excellent agreement. The thermal impedance matrix was evaluated according to the three device layouts, again obtaining virtually thermally decoupled fingers (see Fig. 2 for the 2 fingers layout). This behaviour is confirmed by the self-consistent DC analysis, since the output characteristics, shown in Fig. 6, 7 and 8 for the 2, 4 and 8 emitters layouts, respectively, show the onset of gain collapse for the same value of collector bias voltage. An interpretation of the gain collapse phenomenon as a bifurcation process is described in [8].

Finally, a self-consistent, fully dynamic electro-thermal simulation was carried out, for the bias point $I_B = 0.4, 0.8, 1.6$ mA for the 2, 4 and 8 fingers devices, respectively. The devices were driven in nonlinear operation by adding a base current input tone with amplitude 0.3, 0.6 and 1.2 mA. Fig. 9 shows a comparison of the DC component of the output total collector current as a function of collector bias for the two layouts and for input tones at $f = 1$ MHz and $f = 1$ GHz. A significant dispersion effect both in the device gain and the collapse onset can be observed.

ACKNOWLEDGEMENTS. This work was partly supported by the italian CNR through MADESS II project.

REFERENCES

- [1] W. Liu et al., *The use of base ballasting to prevent the collapse of current gain in AlGaAs/GaAs heterojunction bipolar transistors*, IEEE Trans. El. Dev., p. 245, 1996.
- [2] Ke Lu et al., *Analysis of thermal instability in multi-finger power AlGaAs/GaAs HBTs*, IEEE Trans. Electron Devices, Vol. 43, p. 1799, 1996.
- [3] Y. Zhu et al., *Analytical Model for electrical and thermal transients of self-heating semiconductor devices*, IEEE Trans. Microwave Theory and Techniques, Vol. 46, p. 2258, 1998.
- [4] T. Veijola, *Model for thermal spreading impedance in GaAs MESFETs*, ICECS Tech. Digest, p. 872, 1996.
- [5] P. Leturcq et al., *A new approach to thermal analysis of power devices*, IEEE Trans. El. Dev., Vol. ED-34, p. 1147, 1987.
- [6] R. Anholt, *Electrical and thermal characterization of MESFETs, HEMTs and HBTs*, Artech House, 1995.
- [7] K. S. Kundert et al., *Steady-state methods for simulating analog and microwave circuits*, Kluwer, 1990.
- [8] F. Cappelluti et al., *A new dynamic, self-consistent electro-thermal model of power HBTs and a novel interpretation of thermal collapse loci in multi-finger devices*, CICC Tech. Digest, p. 397, 2001.

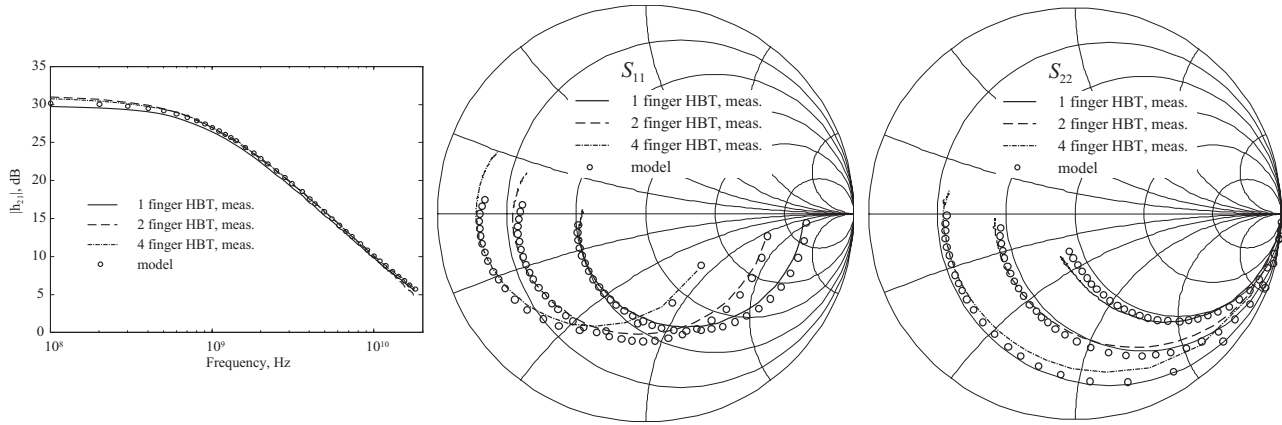


Figure 5: Comparison between the measured and modelled small-signal behaviour for the 1, 2 and 4 finger HBT: magnitude of h_{21} (left), S_{11} (center) and S_{22} (right).

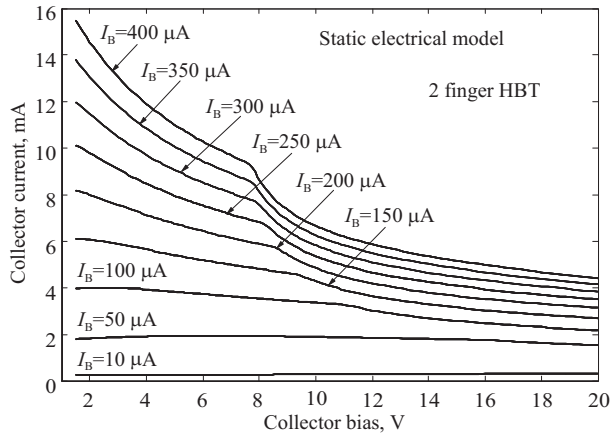


Figure 6: Static (DC) output characteristics for the 2 finger HBT.

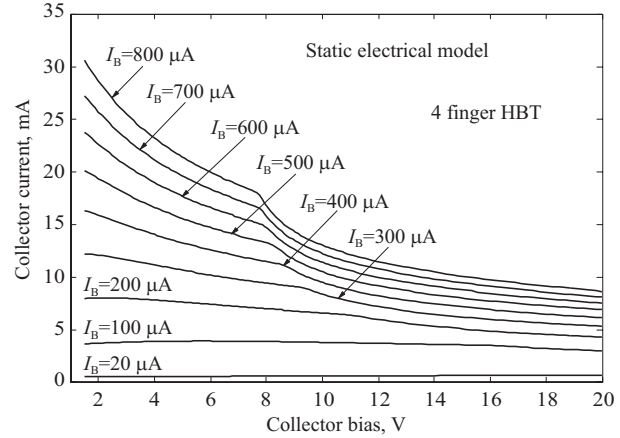


Figure 7: Static (DC) output characteristics for the 4 finger HBT.

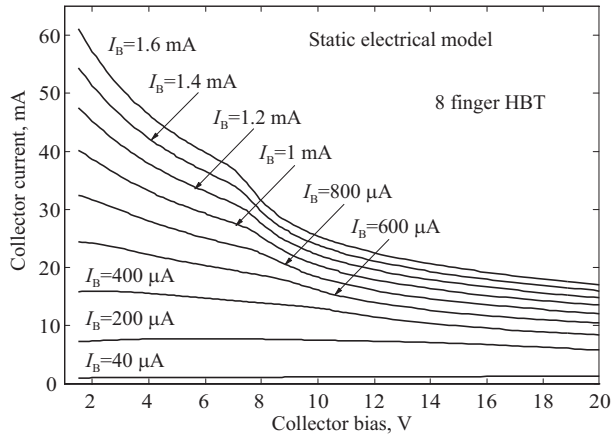


Figure 8: Static (DC) output characteristics for the 8 finger HBT.

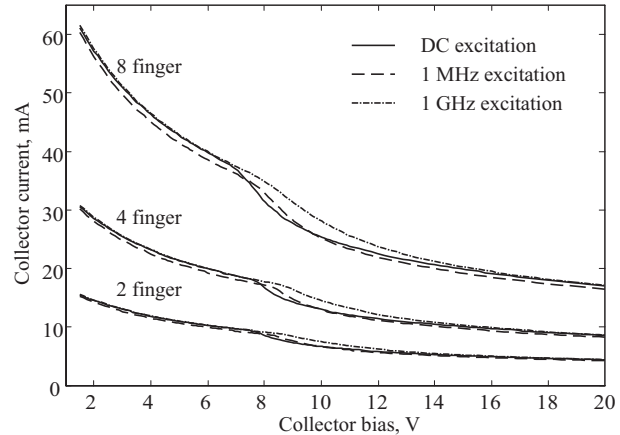


Figure 9: DC component of the dynamic output characteristics compared to the static curve.